



Aqueous Dynamic Covalent Assembly of Molecular Ladders and Grids Bearing Boronate Ester Rungs

Journal:	<i>Polymer Chemistry</i>
Manuscript ID	PY-ART-11-2018-001705.R2
Article Type:	Paper
Date Submitted by the Author:	25-Mar-2019
Complete List of Authors:	Dunn, Megan; University of Michigan, Chemical Engineering Wei, Tao; University of Michigan, Chemical Engineering Zuckermann, Ronald; The Molecular Foundry, Biological Nanostructures Facility Scott, Timothy; University of Michigan, Ann Arbor, Chemical Engineering



Journal Name

ARTICLE

Aqueous Dynamic Covalent Assembly of Molecular Ladders and Grids Bearing Boronate Ester Rungs

Megan F. Dunn,^a Tao Wei,^a Ronald N. Zuckermann,^b and Timothy F. Scott^{a,c,*}Received 00th January 20xx,
Accepted 00th January 20xx

DOI: 10.1039/x0xx00000x

www.rsc.org/

Mimicking the self-assembly of nucleic acid sequences into double-stranded molecular ladders that incorporate hydrogen bond-based rungs, dynamic covalent interactions enable the fabrication of molecular ladder and grid structures with covalent bond-based rungs. Here, we describe the synthesis of boronic acid- and catechol-bearing peptoid oligomers and utilize the dynamic, reversible condensation reaction between these reactive pendant groups to mediate the dynamic covalent assembly of complementary oligomers in aqueous solution, affording both molecular ladders and grids linked by covalent, boronate ester-based rungs. The generation of in-registry molecular ladders with up to six rungs and triplex molecular grids was confirmed by matrix-assisted laser desorption/ionization time-of-flight (MALDI-TOF) mass spectrometry, and the dynamic nature of the condensation reaction was demonstrated by rapid strand displacement with pre-assembled molecular ladders. Additionally, through the use of an indicator displacement assay with alizarin red S (ARS), the boronic acid/catechol binding constant for the formation of molecular ladders was determined.

Introduction

Important examples of self-assembly, such as the formation of lipid bilayers,¹ polypeptide folding,² and nucleic acid hybridization,³ can be found ubiquitously in biological systems. These molecular self-assembly processes often rely upon weak, kinetically-labile intermolecular interactions, such as hydrogen bonding, π stacking, or van der Waals interactions,⁴ to afford a mechanism for rearrangement and error correction. Consequently, the assembled structures can be fragile and susceptible to thermal and mechanical degradation. Several synthetic approaches have been employed to stabilize self-assembled structures *via* post-assembly covalent cross-linking.⁵⁻⁷ Alternatively, the assembly process itself can be mediated by dynamic covalent bond-forming reactions, where the covalent bond connectivity can be reversed or rearranged under specific reaction conditions to effect a mechanism for error correction, thereby directly affording covalently cross-linked assemblies.⁸

A dynamic covalent interaction of particular interest is the reversible, pH-sensitive condensation reaction between boronic acids and diols to yield boronate esters (see Scheme

1). This reaction has been employed extensively in applications ranging from the assembly of macrocycles,⁹ cages,¹⁰ and covalent organic frameworks¹¹ to pH-dependent healable gels¹² and targeted drug delivery vehicles.¹³ Moreover, there has been considerable work into the use of boronic acids for saccharides detection.^{14, 15} Wang et al. have investigated the binding between aryl boronic acids and a library of different diols including many common sugars.^{16, 17} They were able to develop a method using alizarin red S (ARS), a fluorescent diol, to calculate boronic acid/diol binding constants and examine the influence of pH on conjugation. This method has been adapted to demonstrate oligomer cyclization¹⁸ and determine the binding affinity of functionalized polymer strands for a library of diols.¹⁹

In addition to hydrogen bonding between complementary nucleic acid sequences, metal–ligand coordination interactions have been employed to mediate the self-assembly of double-stranded molecular ladders to afford metallosupramolecular ladder structures.²⁰⁻²³ The use of non-symmetric dynamic covalent reactions for paired interactions between complementary oligomeric strands to form molecular ladder structures was first described by the Moore group, who employed Sc(III)-catalysed imine rearrangement for to mediate the self-assembly of complementary *m*-phenylene ethynylene oligomers into *n*-rung molecular ladders, where $n \leq 5$.^{24, 25} We recently described the self-assembly of molecular ladders with up to 16 imine-based rungs in organic solvents *via* Sc(III)-catalysed imine rearrangement,^{26, 27} while the Anslyn group subsequently examined the Vernier-templated assembly of similar structures generated from aldehyde- and hydrazide-

^a Department of Chemical Engineering, University of Michigan, Ann Arbor, MI 48109, US

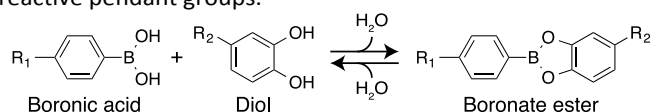
^b Molecular Foundry, Lawrence Berkeley National Laboratory, Berkeley, CA 94720, US

^c Macromolecular Science and Engineering, University of Michigan, Ann Arbor, MI 48109, US

Electronic Supplementary Information (ESI) available: Synthetic procedures, molecular structures, NMR spectra, RP-HPLC traces, and additional mass spectra

bearing peptides.²⁸ Nevertheless, the reversible boronic acid/catechol condensation as a dynamic reaction pair to mediate molecular ladder fabrication lends itself as an orthogonal dynamic covalent interaction²⁹ for oligomer hybridization and enables the assembly itself to proceed rapidly under aqueous conditions,³⁰ thereby mimicking the assembly process and reaction conditions for nucleic acid hybridization and mitigate the formation of kinetically-trapped species that often impedes self-assembly systems mediated by alternative dynamic covalent interactions.^{25, 31}

Here, we employ the dynamic covalent boronic acid/diol interaction to mediate the self-assembly of boronic acid- and catechol-bearing oligomers into molecular ladders incorporating covalent boronate ester rungs. Additionally, by taking advantage of peptoid geometry where adjacent pendant groups are presented on opposite sides of the backbone,³² we describe the fabrication of triplex, 'grid' structures from the co-assembly of three peptoid oligomers, where two strands flank a central core. We also explore the dynamic nature of the system by characterizing the strand rearrangement that proceeds upon addition of a mass-labelled, catechol-bearing peptoid to an already formed molecular ladder. Finally, we examine the binding affinity of the system through competitive binding with alizarin red S (ARS) as a fluorescent diol both quantitatively with peptoid strands that each have one dynamic covalent functional group, and qualitatively for a longer hybridized structure bearing four reactive pendant groups.



Scheme 1. Reversible condensation reaction between a boronic acid and a diol to afford a boronate ester.

Results and Discussion

Dynamic Covalent Assembly of Molecular Ladder and Grid Structures

Peptoids (i.e., poly(N-substituted glycine)s) were employed here as the oligomeric precursor strands for dynamic covalent assembly owing to their ready synthetic accessibility *via* the 'submonomer' solid phase synthetic scheme,³³ enabling the facile incorporation of a variety of pendant functionalities, including reactive boronic acid- and catechol-based functional groups and inert 'spacer' moieties, through the use of primary amine monomers.³⁴ For the pair of dynamic covalent-reactive monomers, the pendant boronic acid and catechol functionalities were protected with acid-labile groups to ensure that they did not participate in deleterious side reactions during the oligomer syntheses. The catechol pendant functionality was incorporated on the peptoid chain *via* acetonide-protected dopamine (Nace), whereas the boronic acid functionality was incorporated through the use of 4-aminomethylphenyl boronic acid pinacol ester (Npbe). Additionally, the inert spacer monomers 2-methoxyethylamine (Nme) and 2-(2-ethoxyethoxyethylamine) (Nee) were

incorporated between each of the dynamic covalent-reactive pendant groups to improve the solubility of both the initial oligomers and the resulting hybridized structure. The dynamic covalent reactants incorporated on the synthesized peptoid strands were either exclusively boronic acid or catechol functional groups to ensure an absence of premature inter-strand reaction that would impede oligomer purification. All of the peptoid oligomers used in this study were generated by solid phase synthesis using an automated peptide synthesizer and were purified by preparative reverse phase high performance liquid chromatography (RP-HPLC). Electrospray ionization (ESI) mass spectrometry was used to verify the molecular weight of the oligomers and analytical RP-HPLC was used to ascertain oligomer purities (Figure S5 and S6).

Boronic acid-bearing peptoid oligomers were initially synthesized as sequences of alternating inert Nme spacer and dynamic covalent Npbe residues, where the number of Npbe residues was varied from 3 to 6. Whereas pinacol ester is widely used as an acid-labile boronic acid protecting group,³⁵ attempts at direct deprotection by treatment with trifluoroacetic acid (TFA) proved inconsistent and often resulted in significant amounts of boronic acid oxidation to the corresponding phenol, adversely affecting yield upon purification. Consequently, we employed a two-step process to effect its removal whereby the boronate ester was initially subject to an on-bead transesterification reaction with diethanolamine,³⁶ efficiently replacing the pinacol group, followed by hydrolysis and simultaneous cleavage of the peptoid from the solid support with TFA and water to afford free peptoids bearing exposed boronic acid residues (i.e., Npba) that were denoted as (NmeNpba)_nNme, where *n* = 3-6. In contrast to the single-step TFA treatment of the pinacol-protected boronic acid during peptoid cleavage, this two-step process avoided oxidation and yielded a more comprehensive cleavage of the pinacol group from the boronate ester. For the complementary, catechol-bearing oligomers, peptoids were synthesized with alternating Nme and Nace monomers, as well as two peptoids that exclusively incorporated Nace residues. The acetonide protecting group were removed by extended treatment with TFA during peptoid cleavage to afford free peptoids bearing the desired catechol functionality, denoted by Ndop.

To illustrate the oligomer hybridization process employed here, a schematic diagram showing the expected self-assembly route of a molecular ladder with six rungs is presented in Figure 1a. Here, co-reaction of complementary precursor oligomers, each incorporating six reactive pendant groups, initially affords a mixture of intermediate ladder species with varying numbers of rungs, species which are annealed out of the mixture as the reaction proceeds owing to the dynamic rearrangement of the generated boronate ester linkages to ultimately form the fully in-registry, six-rung molecular ladder (i.e., Hybrid-6). This hybridization process was experimentally executed by mixing complementary, boronic acid- and catechol-bearing oligomers bearing equal numbers of reactive pendant groups (i.e., (NmeNpba)_nNme and (NmeNdop)_nNme) at a 1:1 stoichiometric ratio in an aqueous solution, the pH of

which was adjusted to 9 by addition of a dilute sodium hydroxide solution to maximize the boronic acid/catechol binding constant.¹⁶ Importantly, these hybridization experiments were performed in an anaerobic environment owing to the susceptibility of the pendant catechol groups to oxygen under alkaline conditions;^{12, 37} indeed, the reaction mixture would progressively turn a pale pink color upon exposure to air, providing a visual indication of catechol oxidation to the corresponding *o*-quinone.^{38, 39} As the forward condensation reaction between a boronic acid and a catechol yields a boronate ester and two water molecules such that the mass of any molecular ladder formed decreases by 36 for each rung generated, MALDI-TOF mass spectrometry was performed in negative mode on aliquots of the crude reaction mixtures after reaction overnight (see Figure 1b) to determine the identity of the products. Hybridization experiments were performed using precursor oligomers bearing from three to six reactive pendant groups and, whereas intermediate ladder species were not identified in any of the reaction mixtures examined, the major peak in each of the MALDI-TOF spectra was assigned as the desired, fully in-registry molecular ladder for the respective reaction mixtures. Notably, positive mode MALDI-TOF mass spectra were also collected on the reaction mixture aliquots (Figure S7, S8, and S9); however, this method was limited to characterizing molecular ladders with five rungs or fewer, owing to poor signal strength for higher molecular weight, boronate ester-bearing species. Nevertheless, the major peak in the spectra for each of the mixtures of oligomers with three to five reactive pendant groups was again identified as the target, in-registry molecular ladder product, supporting the identification as determined by negative mode mass spectrometry. ¹H-NMR spectroscopy proved ill-suited for identification of ladder species as it was unable to discriminate between mixtures of single strands, out-of-registry, and in-registry species (see Figure S12 for ¹H-NMR spectrum of Hybrid-3).

Recent work on peptoid-based, two-dimensional ‘nanosheets’, assembled from amphiphilic sequences of ionic and hydrophobic residues revealed that their constituent peptoid chains adopt a ‘ Σ -strand’ conformation, where adjacent pendant groups are presented on opposite sides of the peptoid backbone.³² Moreover, the chemical and mechanical stability of these structures was effected by the post-assembly covalent cross-linking of their hydrophobic core. Inspired by this work and having successfully realized the hybridization of complementary oligomers to afford dimeric, molecular ladder structures, we employed dynamic covalent assembly to afford finite molecular grids from the interaction of multiple precursor peptoid oligomers in a preliminary effort towards the fabrication of inherently cross-linked nanosheets and ribbons. To ensure their facile characterization by mass spectrometry, the assembly of these grids was designed to proceed between two boronic acid-bearing oligomers flanking a catechol-bearing core to afford designed well-defined, three-stranded structures, denoted here as 3×3 and 3×4 grids to represent the 3 strands with either 3 or 4 dynamic covalent interactions per oligomer pair. Whereas the sequences of the

flanking strands maintain the use of alternating dynamic covalent-reactive and inert spacer residues, the triplex cores were composed exclusively of residues bearing reactive pendant groups. Thus, triplex grids were assembled by adding 2 equivalents of a boronic acid-bearing peptoid ((NmeNbor)_nNme) to a catechol-bearing hexafunctional peptoid (Ndop_{2n}), as shown in Figure 1c. MALDI-TOF mass spectrometry was again employed to confirm the formation of the target 3×3 and 3×4 grid structures (Figure 1d). Our previous work on Vernier-templated dynamic covalent assembly examined the concurrent interaction of greater than two oligomeric precursor strands to afford long, linear molecular ladders;²⁶ nevertheless, the multi-oligomer molecular grids described here demonstrate an approach to achieve assembly perpendicular to the precursor oligomer axes to yield wide, non-linear structures, suggesting the potential for the fabrication of covalently-bonded, raft-like nanosheets composed of many linear oligomers.

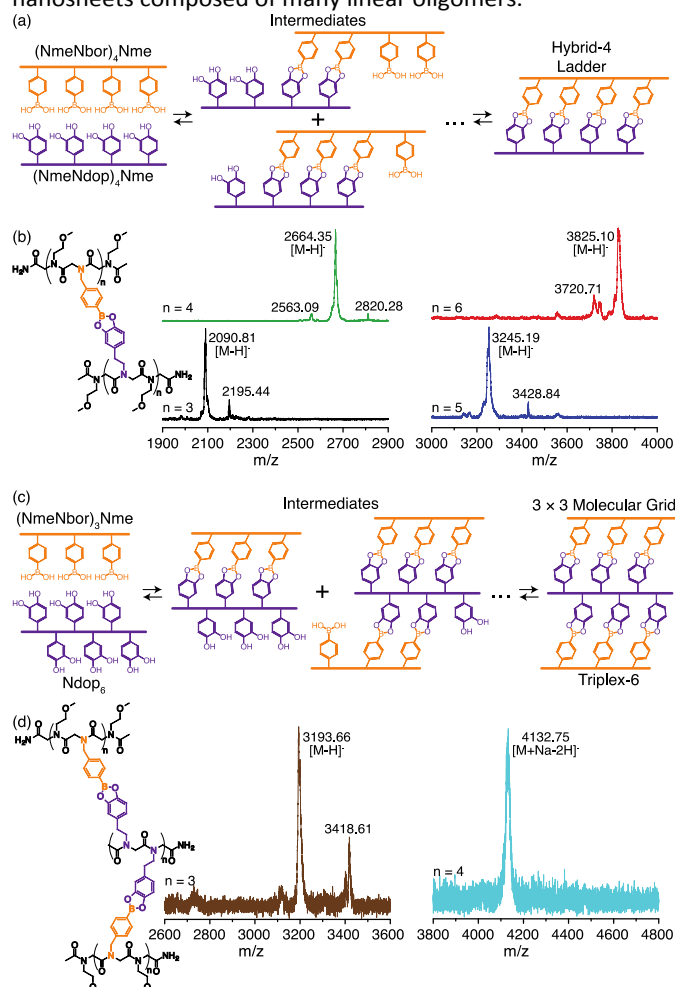


Figure 1. Dynamic covalent assembly of boronate ester-based molecular ladders and grids. a) Schematic diagram showing the anticipated dimerization of complementary, boronic acid- and catechol-bearing oligomers to afford in-registry molecular ladders. b) Negative mode MALDI-TOF mass spectra confirming the formation of peptoid-based molecular ladders bearing from 3 to 6 boronate ester rungs (molecular structures as shown). c) Schematic diagram showing the anticipated hybridization of two boronic acid-bearing oligomers with a catechol-bearing core oligomer to

afford a triplex grid. d) Negative mode MALDI-TOF mass spectra of assembled 3×3 and 3×4 grid structures (molecular structures as shown).

Molecular Ladder Scrambling by Strand Displacement

In order to explore the dynamic nature of the boronate ester-based molecular ladders and grids assembled from boronic acid- and catechol-bearing precursors, a mass-labelled, catechol-functionalized peptoid strand was added to an existing dimeric hybrid and the strand rearrangement and displacement by transesterification monitored (see Figure 2a). Whereas the initial hybrid (hybrid-3) incorporated the Nme spacer for both boronic acid- and catechol-bearing precursor oligomers (i.e., (NmeNpba)₃Nme and (NmeNdop)₃Nme, respectively), the catechol-bearing peptoid added to the hybrid solution was mass-labelled by employing Neee as the spacer residue owing to its a higher molecular weight than Nme. Thus, exchange of the catechol-bearing (NmeNdop)₃Nme strand in the parent molecular ladder for (NeeeNdop)₃Neee yields a daughter ladder with a higher molecular weight than its parent and readily differentiated by mass spectrometry. The MALDI-TOF spectrum of the initial reaction mixture of (NmeNdop)₃Nme and (NmeNpba)₃Nme (Figure 2b, bottom) shows a single peak at 2105.97, attributable to the Na⁺ ionization of the initial hybridized molecular ladder structure generated by the interaction of the two peptoid strands; however, upon addition of the (NeeeNdop)₃Neee strand, two distinct product peaks in the positive mode MALDI-TOF spectrum of the reaction mixture are observed (Figure 2b, top), one at 2105.97 corresponding to the initial, parent hybrid, and a second pair at 2336.1 and 2346.3, corresponding to the Na⁺ and CH₃OH+H⁺ ionizations, respectively, of a daughter molecular ladder composed of (NmeNpba)₃Nme and (NeeeNdop)₃Neee peptoid strands. The mass spectrum showing both the parent and daughter hybrids (i.e., Figure 2b, top) was collected after overnight incubation; however, a peak attributable to the daughter ladder was observable in mass spectra collected within minutes after adding the (NeeeNdop)₃Neee strand, suggesting that, in contrast to earlier work in our lab with imine-forming tetramers,²⁶ this dynamic rearrangement proceeded rapidly. Whereas progress of the generation and scrambling reactions for the imine-bearing molecular ladders could be readily monitored by employing MALDI-TOF on reaction mixture aliquots, this time-resolved method proved ill-suited for quantitatively following either the initial assembly or rearrangement of boronate ester-based molecular ladders owing to their rapid reaction rates. Notably, whereas self-assembly processes mediated by dynamic covalent reactions tend to become kinetically-trapped even for systems with moderate numbers of interactions,^{25, 31} rapid connectivity rearrangement such as that observed here advances convergence of the system towards thermodynamic equilibrium, thereby suppressing kinetic trapping and enabling synthetic success.

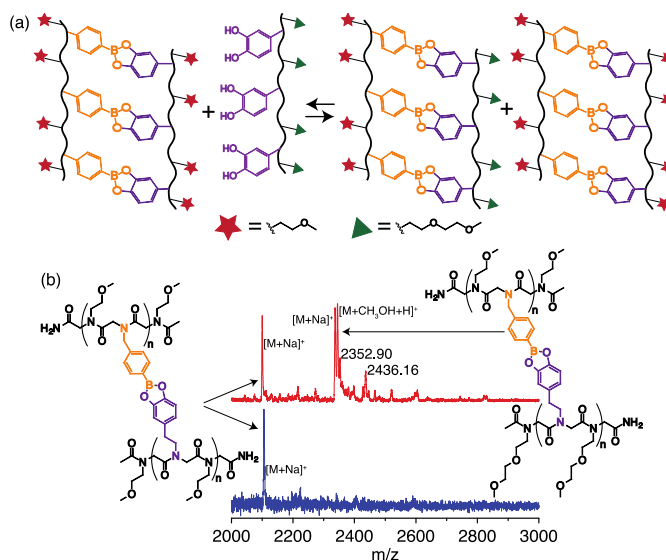


Figure 2. Molecular ladder strand displacement. a) Schematic diagram of strand rearrangement where the fully-formed hybrid-3, assembled from oligomers incorporating the inert Nme spacer residue (denoted by a star), is reacted with (NeeeNdop)₃Neee, a peptoid oligomer bearing the Neee spacer residue (denoted by a triangle). Upon displacement of the original, Nme-bearing (NmeNdop)₃Nme by the introduced, Neee-bearing oligomer, the mixture achieves a new equilibrium state that includes the original hybrid-3, the newly-hybridized structure, hybrid-E3, and both catechol-bearing peptoids as free oligomers. b) Positive mode MALDI-TOF spectra of (bottom) the initial reaction mixture incorporating the hybrid-3 structure ($m/z = 2105.97 [M+Na]^+$), and (top) the reaction mixture after the addition of (NeeeNdop)₃Neee, incorporating both the initially-formed hybrid-3 ($m/z = 2105.97 [M+Na]^+$) and the newly-formed hybrid-E3 ($m/z = 2336.19 [M+Na]^+$ and $m/z = 2346.3 [M+CH_3OH+H]^+$).

Monitoring Transesterification Rate and Binding Constant

Given the importance of high reaction rates to suppress kinetically-trapped species and thereby ensuring self-assembly success, we further explored strategies to ascertain molecular ladder transesterification rates. Thus, an indicator displacement assay⁴⁰ was performed by using ARS, a diol that affords an observably lower fluorescence signal in free solution than when bound to a boronic acid (Figure 3a).⁴¹ A plate reader was used to obtain a kinetic scan that compared the change in fluorescent intensity ($\lambda_{exc} = 485 \pm 20$ nm and $\lambda_{em} = 620 \pm 20$ nm) between a control sample that contained only (NmeNpba)₄Nme bound to ARS and a sample where 10 equivalents of (NmeNdop)₄Nme was added to the ARS bound (NmeNpba)₄Nme. Although the kinetic scan began immediately upon addition of (NmeNdop)₄Nme to the sample, the samples had already plateaued before the first time point was completed (see Figure S13), suggesting that the samples were at equilibrium before the readings were taken (i.e., less than 10 seconds after mixing), a timescale consistent with literature values indicating that the process approaches equilibrium within 5–10 s.⁴² Nevertheless, the rapid rate of this exchange reaction allowed for equilibrium to be achieved quickly enabling the binding constant between peptoids bearing boronic acid and catechol pendant groups to be readily evaluated. Here, the binding constant between Nme₂-Ndop-Nme₂ and Nme₂-Ndpba-Nme₂ was determined to serve

as a proxy for the relationship between each of the complementary peptoid structures. Briefly, varying equivalents of boronic acid peptoid was incubated with a fixed concentration of ARS to first establish an equilibrium-binding constant, K_{eq} . This relationship followed a logarithmic curve (Figure 3c) that plateaued at approximately 10 equivalents of the boronic acid peptoid. In contrast, increasing equivalents of the catechol oligomer were added to the boronic acid oligomer bound to ARS that yielded an exponential decay of fluorescence intensity (Figure 3d). This trend can be attributed to the release of ARS back into solution as the catechol oligomer starts to displace the bound ARS and dimerize with the boronic acid peptoid. The exchange reaction between the ARS and catechol oligomer further demonstrates the dynamic nature of this system through the reversible formation of boronate esters. The same experiments were repeated with complementary tetramer peptoids, (NmeNdp)₄Nme and (NmeNpba)₄Nme (Figure S14). This was a qualitative test to demonstrate that the longer peptoid ladders follow a similar trend to the one functional group peptoids.

The Benesi-Hildebrand method,⁴³ a mathematical method for determining equilibrium constants of non-bonding interactions, was adapted for use with fluorescence data and used to determine the equilibrium constant, K_{PBA} , of the boronic acid and ARS complex. The analysis followed a method outlined by Gennari et al.¹⁹ where the inverse of the change in fluorescent intensity (ΔI_f) was plotted against the inverse of the boronic acid concentration ($[PBA]$), and K_{PBA} was determined by fitting the line and dividing the intercept by the slope following equation (1). In this equation, $\Delta k p_0$ is a constant that is dependent on the laser power and the intrinsic fluorescence, and $[A]_0$ is the total concentration of ARS. This yielded a K_{PBA} value of 2664 M⁻¹.

$$\frac{1}{\Delta I_f} = \left(\Delta k p_0 [A]_0 K_{PBA} \right)^{-1} \frac{1}{[PBA]} + \left(\Delta k p_0 [A]_0 \right)^{-1} \quad (1)$$

The equilibrium constant between the boronic acid and catechol peptoids can be expressed by the equilibrium reaction shown in equation 2 where A is the ARS, B is the boronic acid-bearing oligomer, and C is the catechol-bearing oligomer. The equilibrium of this reaction, K (equation 3), can be shown as the ratio of the formation constants for the two boronate esters (AB and CB). This equation can be further expanded to be represented in terms of the concentration of free ARS, $[A]$ (equation 4).



$$K = \frac{[A][CB]}{[AB][C]} = \frac{K_{DOP}}{K_{PBA}} \quad (3)$$

$$K = \frac{[A]([PBA] - [AB])}{([A]_0 - [A])[C]} \quad (4)$$

$$K = \frac{[A]([PBA] - [A]_0 + [A])}{([A]_0 - [A])([DOP] - [PBA] + ([A]_0 - [A]))} \quad (5)$$

The $[A]$ for each of the different catechol equivalents was calculated by determining the percentage of free ARS by the change in fluorescent intensity and multiplying that by the initial concentration, $[A]_0$. Once K is determined (Equation 5), it can be multiplied by K_{PBA} to determine K_{DOP} , the equilibrium constant for the boronate ester reaction. The K_{DOP} values for the various catechol concentrations ($[DOP]$) were averaged to yield a binding constant of 276 M⁻¹, approximately an order of magnitude lower than monomeric binding between phenylboronic acid and catechol.¹⁶ Although the Benesi-Hildebrand method is effective for determining binding constants for 1:1 interactions, quantitatively characterizing a sample that has multiple possible interactions, such as the tetramer peptoids where there are four boronic acid functional groups that can bind with ARS each interaction eliciting a change in the fluorescent intensity, is more challenging. Indeed, the multivalent binding between the peptoid strands likely contribute to a stronger affinity than single interaction when considering the effective local functional group concentration, a phenomena prevalent in biological systems.⁴⁴ The different sites could follow this so-called "cluster effect" owing to the proximity of the interactions along the peptoid backbone where the binding of one group will lead to increased localized concentration of the unreacted functional groups resulting in strong binding affinity in the remaining groups.

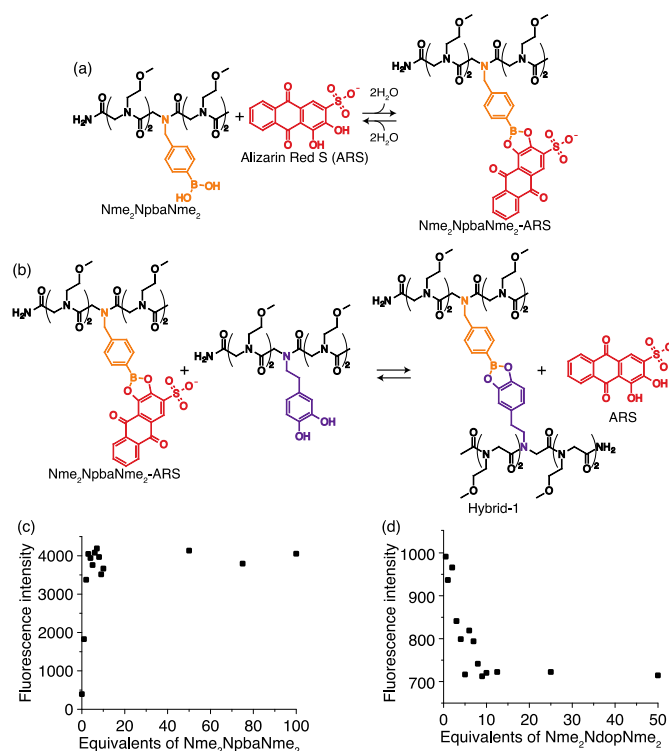


Figure 3. Competitive binding between boronic acid- and catechol-bearing peptoids and the diol fluorophore, ARS. Schematic diagrams showing a) the binding between $\text{Nme}_2\text{NpbaNme}_2$ and ARS, and b) the displacement of ARS bound to $\text{Nme}_2\text{NpbaNme}_2$ when $\text{Nme}_2\text{NdopNme}_2$ is introduced to the system. c) Increase in fluorescent intensity as increasing equivalents of $\text{Nme}_2\text{NpbaNme}_2$ bind with ARS. d) Changes in fluorescent intensity as $\text{Nme}_2\text{NdopNme}_2$ displaces ARS, bound to $\text{Nme}_2\text{NpbaNme}_2$, and is released into solution.

Conclusions

We have demonstrated the successful dynamic covalent assembly of molecular ladders and grids incorporating boronate ester rungs in aqueous solution through the hybridization of complementary, peptoid-based precursor oligomers bearing boronic acid and catechol pendant groups. Ladders with up to 6 rungs were assembled in alkaline aqueous solution and identified by mass spectrometry, as were 3×3 and 3×4 molecular grid structures composed of catechol-functionalized peptoid cores flanked by boronic acid-bearing strands. Strand rearrangement by transesterification between a fully formed, hybridized structure and a competing, mass-labelled single-stranded oligomer demonstrated the rapid dynamic nature of the esterification. Although an indicator displacement assay between boronic acid- and catechol-bearing peptoids and the diol fluorophore, ARS, was ineffective in monitoring the rapid transesterification reaction, it provided sufficient data to determine a binding constant for this system of 276 M^{-1} using the changes in fluorescent intensity of solutions containing ARS and dynamic covalent oligomers. The detailed knowledge of the affinity between our peptoid-based oligomers informs reaction conditions necessary to ultimately build more complex molecular architectures. This work establishes a route towards the self-assembly of complex and robust biomimetic nanostructures.

Conflicts of interest

There are no conflicts of interest to declare.

Acknowledgements

This work was supported by the U.S. Department of Energy, Office of Science, Basic Energy Sciences, under Award # DE-SC0012479 and the National Science Foundation Graduate Research Fellowship Program. Additionally, work at the Molecular Foundry was supported by the Office of Science, Office of Basic Energy Sciences, of the U.S. Department of Energy under Contract No. DE-AC02-05CH11231. We would like to thank Mark A. Kline and Michael Connolly for instrumentation assistance at the Molecular Foundry. We would also like to thank Samuel C. Leguizamon for assistance with mass spectrometry.

Notes and references

1. J. M. Schnur, *Science*, 1993, **262**, 1669-1676.
2. M. J. Gething and J. Sambrook, *Nature*, 1992, **355**, 33-45.
3. M. Zuker, *Nucleic Acids Res.*, 2003, **31**, 3406-3415.
4. S. G. Zhang, *Nat. Biotechnol.*, 2003, **21**, 1171-1178.
5. A. Rajendran, M. Endo, Y. Katsuda, K. Hidaka and H. Sugiyama, *J. Am. Chem. Soc.*, 2011, **133**, 14488-14491.
6. H. O. Abdallah, Y. P. Ohayon, A. R. Chandrasekaran, R. J. Sha, K. R. Fox, T. Brown, D. A. Rusling, C. Mao and N. C. Seeman, *Chem. Commun.*, 2016, **52**, 8014-8017.
7. K. Maeda, L. Hong, T. Nishihara, Y. Nakanishi, Y. Miyauchi, R. Kitaura, N. Ousaka, E. Yashima, H. Ito and K. Itami, *J. Am. Chem. Soc.*, 2016, **138**, 11001-11008.
8. S. J. Rowan, S. J. Cantrill, G. R. L. Cousins, J. K. M. Sanders and J. F. Stoddart, *Angew. Chem., Int. Ed.*, 2002, **41**, 898-952.
9. N. Christinat, R. Scopelliti and K. Severin, *J. Org. Chem.*, 2007, **72**, 2192-2200.
10. N. Christinat, R. Scopelliti and K. Severin, *Angew. Chem., Int. Ed.*, 2008, **47**, 1848-1852.
11. A. P. Cote, A. I. Benin, N. W. Ockwig, M. O'Keeffe, A. J. Matzger and O. M. Yaghi, *Science*, 2005, **310**, 1166-1170.
12. L. H. He, D. E. Fullenkamp, J. G. Rivera and P. B. Messersmith, *Chem. Commun.*, 2011, **47**, 7497-7499.
13. Y. P. Li, W. W. Xiao, K. Xiao, L. Berti, J. T. Luo, H. P. Tseng, G. Fung and K. S. Lam, *Angew. Chem., Int. Ed.*, 2012, **51**, 2864-2869.
14. X. T. Zhang, G. J. Liu, Z. W. Ning and G. W. Xing, *Carbohydr. Res.*, 2017, **452**, 129-148.
15. R. Nishiyabu, Y. Kubo, T. D. James and J. S. Fossey, *Chem. Commun.*, 2011, **47**, 1106-1123.
16. J. Yan, G. Springsteen, S. Deeter and B. H. Wang, *Tetrahedron*, 2004, **60**, 11205-11209.
17. G. Springsteen and B. H. Wang, *Tetrahedron*, 2002, **58**, 5291-5300.
18. S. Chirayil and K. J. Luebke, *Tetrahedron Lett.*, 2012, **53**, 726-729.
19. A. Gennari, C. Gujral, E. Hohn, E. Lallana, F. Cellési and N. Tirelli, *Bioconjugate Chem.*, 2017, **28**, 1391-1402.
20. P. N. Taylor and H. L. Anderson, *J. Am. Chem. Soc.*, 1999, **121**, 11538-11545.
21. T. E. O. Screen, J. R. G. Thorne, R. G. Denning, D. G. Bucknell and H. L. Anderson, *J. Am. Chem. Soc.*, 2002, **124**, 9712-9713.
22. M. B. Coppock, J. R. Miller and M. E. Williams, *Inorg. Chem.*, 2011, **50**, 949-955.
23. J. Adisojoso, Y. Li, J. Liu, P. N. Liu and N. Lin, *J. Am. Chem. Soc.*, 2012, **134**, 18526-18529.
24. C. S. Hartley, E. L. Elliott and J. S. Moore, *J. Am. Chem. Soc.*, 2007, **129**, 4512-4513.
25. E. L. Elliott, C. S. Hartley and J. S. Moore, *Chem. Commun.*, 2011, **47**, 5028-5030.
26. T. Wei, J. H. Jung and T. F. Scott, *J. Am. Chem. Soc.*, 2015, **137**, 16196-16202.
27. T. Wei, J. C. Furgal, J. H. Jung and T. F. Scott, *Polym. Chem.*, 2017, **8**, 520-527.
28. J. F. Reuther, J. L. Dees, I. V. Kolesnichenko, E. T. Hernandez, D. V. Ukraintsev, R. Guduru, M. Whiteley and E. V. Anslyn, *Nat. Chem.*, 2018, **10**, 45-50.
29. D.-W. Zhang and Z.-T. Li, in *Dynamic Covalent Chemistry*, eds. W. Zhang and Y. Jin, John Wiley & Sons Ltd, 2017, DOI: doi:10.1002/9781119075738.ch5, ch. 5, pp. 207-249.
30. Y. Furikado, T. Nagahata, T. Okamoto, T. Sugaya, S. Iwatsuki, M. Inamo, H. D. Takagi, A. Odani and K. Ishihara, *Chem.-Eur. J.*, 2014, **20**, 13194-13202.

31. S. Lee, A. Yang, T. P. Money Penny and J. S. Moore, *J. Am. Chem. Soc.*, 2016, **138**, 2182-2185.
32. J. R. Edison, R. K. Spencer, G. L. Butterfoss, B. C. Hudson, A. I. Hochbaum, A. K. Paravastu, R. N. Zuckermann and S. Whitelam, *Proc. Natl. Acad. Sci. U. S. A.*, 2018, **115**, 5647-5651.
33. R. N. Zuckermann, J. M. Kerr, S. B. H. Kent and W. H. Moos, *J. Am. Chem. Soc.*, 1992, **114**, 10646-10647.
34. K. Kirshenbaum, A. E. Barron, R. A. Goldsmith, P. Armand, E. K. Bradley, K. T. Truong, K. A. Dill, F. E. Cohen and R. N. Zuckermann, *Proc Natl Acad Sci U S A*, 1998, **95**, 4303-4308.
35. Q. I. Churches and C. A. Hutton, in *Boron Reagents in Synthesis*, ed. A. Coca, Amer Chemical Soc, Washington, 2016, vol. 1236, pp. 357-377.
36. J. Sun, M. T. Perfetti and W. L. Santos, *J. Org. Chem.*, 2011, **76**, 3571-3575.
37. S. Wu, W. Waugh and V. J. Stella, *J. Pharm. Sci.*, 2000, **89**, 758-765.
38. H. Jackson and L. P. Kendal, *Biochem. J.*, 1949, **44**, 477-487.
39. J. Yang, V. Saggiomo, A. H. Velders, M. A. C. Stuart and M. Kamperman, *PLoS One*, 2016, **11**, 17.
40. B. T. Nguyen and E. V. Anslyn, *Coord. Chem. Rev.*, 2006, **250**, 3118-3127.
41. G. Springsteen and B. H. Wang, *Chem. Commun.*, 2001, DOI: 10.1039/b104895n, 1608-1609.
42. J. W. Tomsho and S. J. Benkovic, *J. Org. Chem.*, 2012, **77**, 2098-2106.
43. H. A. Benesi and J. H. Hildebrand, *J. Am. Chem. Soc.*, 1949, **71**, 2703-2707.
44. J. D. Badjic, A. Nelson, S. J. Cantrill, W. B. Turnbull and J. F. Stoddart, *Accounts Chem. Res.*, 2005, **38**, 723-732.